RESEARCH ARTICLE

Antibiotic-Driven Dysbiosis Mediates Intraluminal Agglutination and Alternative Segregation of *Enterococcus faecium* from the Intestinal Epithelium

Antoni P. A. Hendrickx,[a] Janetta Top,[a] Jumamurat R. Bayjanov,[a] Hans Kemperman,[b] Malbert R. C. Rogers,[a] Fernanda L. Paganelli,[a] Marc J. M. Bonten,[a] Rob J. L. Willems[a]

Department of Medical Microbiology, University Medical Center Utrecht, Utrecht, The Netherlands[a]; Clinical Chemistry and Hematology, University Medical Center Utrecht, Utrecht, The Netherlands[b]

ABSTRACT **The microbiota of the mammalian gastrointestinal tract is a complex ecosystem of bacterial communities that continuously interact with the mucosal immune system. In a healthy host, the mucosal immune system maintains homeostasis in the intestine and prevents invasion of pathogenic bacteria, a phenomenon termed colonization resistance. Antibiotics create dysbiosis of microbiota, thereby decreasing colonization resistance and facilitating infections caused by antibiotic-resistant bacteria. Here we describe how cephalosporin antibiotics create dysbiosis in the mouse large intestine, allowing intestinal outgrowth of antimicrobial-resistant *Enterococcus faecium*. This is accompanied by a reduction of the mucus-associated gut microbiota layer, colon wall, and Muc-2 mucus layer. *E. faecium* agglutinates intraluminally in an extracellular matrix consisting of secretory IgA (sIgA), polymeric immunoglobulin receptor (pIgR), and epithelial cadherin (E-cadherin) proteins, thereby maintaining spatial segregation of *E. faecium* from the intestinal wall. Addition of recombinant E-cadherin and pIgR proteins or purified IgA to enterococci *in vitro* mimics agglutination of *E. faecium in vivo*. Also, the Ca^{2+} levels temporarily increased by 75% in feces of antibiotic-treated mice, which led to deformation of E-cadherin adherens junctions between colonic intestinal epithelial cells and release of E-cadherin as an extracellular matrix entrapping *E. faecium*. These findings indicate that during antibiotic-induced dysbiosis, the intestinal epithelium stays separated from an invading pathogen through an extracellular matrix in which sIgA, pIgR, and E-cadherin are colocalized. Future mucosal vaccination strategies to control *E. faecium* or other opportunistic pathogens may prevent multidrug-resistant infections, hospital transmission, and outbreaks.**

IMPORTANCE **Infections with antibiotic-resistant enterococci are an emerging worldwide problem because enterococci are resistant to most of the antibiotics used in hospitals. During antibiotic treatment, the normal bacteria are replaced by resistant enterococci within the gut, from which they can spread and cause infections. We studied antibiotic-mediated intestinal proliferation of multidrug-resistant *Enterococcus faecium* and the effects on intestinal architecture. We demonstrated that antibiotics allow proliferation of *E. faecium* in the gut, alter the mucus-associated gut bacterial layer, and reduce the colon wall, mucus thickness, and amount of Muc-2 protein. *E. faecium* is agglutinated in the intestine in a matrix consisting of host molecules. We hypothesize that this matrix maintains a segregation of *E. faecium* from the epithelium. Understanding the processes that occur in the gut during antibiotic treatment may provide clues for future mucosal vaccination strategies to control *E. faecium* or other multidrug-resistant opportunistic pathogens, thereby preventing infections, hospital transmission, and outbreaks.**

Received 5 August 2015 **Accepted** 15 October 2015 **Published** 10 November 2015

Citation Hendrickx APA, Top J, Bayjanov JR, Kemperman H, Rogers MRC, Paganelli FL, Bonten MJM, Willems RJL. 2015. Antibiotic-driven dysbiosis mediates intraluminal agglutination and alternative segregation of *Enterococcus faecium* from the intestinal epithelium. mBio 6(6):e01346-15. doi:10.1128/mBio.01346-15.

Editor Fernando Baquero, Ramón y Cajal University Hospital

Address correspondence to Antoni P. A. Hendrickx, A.P.A.Hendrickx-4@umcutrecht.nl.

In a healthy mammalian host, the gastrointestinal microbiota is essential for energy harvest, metabolism of indigestible nutrients, and colonization resistance, a defense mechanism against invading pathogens. The microbiota also determines intestinal architecture, modulates intestinal barrier function, and educates the mucosal innate immune system (1–4). These intestinal barrier defenses include physical separation by a 50-μm-thick mucus layer, junctions between intestinal epithelial cells (IECs), and secretion of antimicrobial peptides (C-type lectins such as Reg3γ) and secretory IgA (sIgA) by IECs (5–9) and protect the host from severe life-threatening inflammatory responses and dissemination of the microbial and luminal contents into the lamina propria (10). Vital components of the IEC monolayer are tight junctions, desmosomes, and adherens junctions between cells (11, 12). Adherens junctions are formed by epithelial cadherin (E-cadherin), a Ca^{2+}-dependent cell-cell adhesion glycoprotein. The N-terminal extracellular ectodomain of E-cadherin is expressed on the apical side of the lateral membrane of IECs, where it interacts with an E-cadherin molecule of a neighboring cell (13, 14). Mucin-2 is an O-linked glycoprotein and is produced by goblet cells to establish the net-like mucus layer (15, 16) of which the outer colonic mucus layer is colonized by bacteria, while the inner mucus layer is de-

void of microbes (17, 18). Mucus forms a separation barrier, and IgA^+ plasma cells produce sIgA in the lamina propria and have an essential role in separating microbiota from the host by immune exclusion, by limiting adhesion to and invasion of the epithelium by microbiota by coating bacterial surfaces and agglutinating bacterial cells (7, 19–21). sIgA binds to the polymeric immunoglobulin receptor (pIgR), a glycoprotein expressed basolaterally on polarized secretory IECs (22–24). sIgA complexes (pIgR-sIgA-J chain), as well as unoccupied pIgR, are internalized into the IEC and transported to the apical surface, where the extracellular part of pIgR is cleaved, leading to release of sIgA and unbound pIgR into the lumen (25–27). Free pIgR has innate immune functions similar to those of sIgA, and bound to IgA, it protects sIgA from proteolytic degradation by microbial proteases in the lumen (28). Perturbation of the intestinal microbiota can deregulate intestinal homeostasis, decrease colonization resistance, and facilitate outgrowth of antibiotic-resistant pathogens (1). Multidrug-resistant *Enterococcus faecium* has emerged as an important cause of hospital-acquired infections in debilitated patients and can become the dominant intestinal species when hospitalized patients receive antibiotics (29–31). Antibiotics diminish intestinal Gram-negative bacteria and result in downregulated expression of the antimicrobial peptide Reg3γ, facilitating outgrowth of *E. faecium* (32). Consequently, the intestines of these patients represent a reservoir from which *E. faecium* can spread and potentially cause infections of the urinary tract, bloodstream, and surgical sites (29). Antibiotic treatment can also alter intestinal pathology (33–35). For instance, metronidazole altered the microbiota and goblet cell function, leading to a reduction of *mucin-2* expression and reduction of the protective mucus layer (36). An altered microbiota, accompanied by decreased levels of Reg3γ, and a thinned mucus layer, reduces the defensive barrier and immune homeostasis. We therefore investigated the intestinal architecture of mice during antibiotic-induced perturbation of the microbiota and subsequent outgrowth of two resistant *E. faecium* isolates in two different animal experiments. We showed that intestinal dysbiosis was accompanied by a reduced mucus separation barrier and enhanced intraluminal agglutination of *E. faecium* in a matrix consisting of sIgA, pIgR, and E-cadherin. We hypothesize that this matrix contributes to the segregation of *E. faecium* from the intestinal epithelium when the mucus layer is reduced.

RESULTS

Antibiotics cause dysbiotic outgrowth of resistant *E. faecium*. To mimic dysbiotic outgrowth of a multiresistant opportunistic pathogen, we treated mice with antibiotics and orally administered antibiotic-resistant *E. faecium* strain E980 (four mice per group) or E1162 (four mice per group) and inoculated untreated animals with E980 or E1162 (four mice per group; thus, eight mice). Control groups were either left untreated (0.9% NaCl; three mice) or treated with antibiotics only (three mice). This experiment was repeated with an additional two mice per group to increase the total number of mice per group and confirm the imaging results (see below) (Fig. 1a). In the groups receiving antibiotics (eight mice), strain E1162 reached ~10×10^{10} bacteria/g of feces and strain E980 reached ~5×10^5 bacteria/g of feces on day 1, and both isolates stably colonized the mouse gut at ~10×10^{10} bacteria/g of feces from day 3 until day 10 (Fig. 1b). Strain E980 or E1162 also stably colonized the guts of untreated mice for 10 days, albeit at lower levels (~1×10^5 bacteria/g of feces) than antibiotic-treated mice. No *E. faecium* was cultured from either control group. Enumeration of CFU from homogenates of the duodenum, jejunum, ileum, cecum, and colon detected colonization by enterococci of the small intestines (10^3 to 10^4 CFU/g of tissue) and in the ceca and colons (10^5 CFU/g of tissue) of animals not receiving antibiotics (Fig. 1c). The level of colonization was 100× to 10,000× higher in the small intestines (10^5 to 10^8 CFU/g of tissue), ceca, and colons (10^{10} CFU/g of tissue) of antibiotic-treated animals. To confirm *Enterococcus*-specific outgrowth, bacterial diversity was determined on the basis of 16S rRNA gene profiling from feces from day −2 until day 10 (Fig. 1d). On day −2, the microbial composition was similar in all groups. The eight major taxa in these groups were *Clostridiales* (2.2 to 25.8% of all sequences), *Lactobacillaceae* (0.7 to 62.4%), *Bacteroidales* (15.9 to 78.7%), *Prevotellaceae* (0.2 to 9.8%), *Ruminococcaceae* (0.4 to 7.3%), *Desulfovibrionaceae* (0.1 to 7.7%), *Bacteroidaceae* (0.2 to 7.2%), and *Coriobacteriaceae* (0.9 to 17.9%). The composition remained stable in the untreated control mice from day −2 until day 10. Animals administered antibiotics only and not receiving *E. faecium* had a greatly diminished microbiota. In contrast, in animals treated with antibiotics and inoculated with *E. faecium* E980 or E1162, the microbiota was dominated by *Enterococcus* bacteria (59.2 to 99.8% and 97.2 to 99.9%, respectively) from day 1 until day 10, indicating that cephalosporin antibiotics led to dysbiotic proliferation of *E. faecium* in the large intestine. Alignment of fecal 16S rRNA gene sequences to *E. faecium* 16S rRNA gene sequences demonstrated that *E. faecium* was the dominant species from day 1 until day 10 (see Fig. S1 in the supplemental material) and that the *Enterococcaceae* family bacteria detected on day 0 in mice that received antibiotics and E980 or E1162 were *E. gallinarum*. This was confirmed by a specific PCR reaction of the *E. faecium ddl* housekeeping gene of DNA extracted from fecal samples.

Antibiotics drive alteration of intestinal architecture in mice. Detailed visualization of the changes in intestinal architecture was performed by Gram staining of Carnoy's solution-fixed and formalin-fixed colon tissue of animals sacrificed on days 1 and 10 from two independent animal experiments. This revealed similar results on both days 1 and 10. Thick layers of microbiota were observed on the apical side of the epithelium of untreated mice ($n = 4$; 99.7 to 115 μm, days 1 and 10) and untreated mice inoculated with either E980 ($n = 2$; 105 μm) or E1162 ($n = 4$; 104.8 to 161 μm) on days 1 and 10 (Fig. 2a and b; see Fig. S2 in the supplemental material). Interestingly, this layer was larger in untreated animals inoculated with E1162 than in untreated animals. The microbiota layer was reduced significantly (133×) in animals treated with antibiotics ($n = 4$; 0.89 μm; $P = 0.0001$) and in animals treated with antibiotics and inoculated with E980 ($n = 2$; 32 μm) or E1162 ($n = 4$; ~1 to 40 μm; $P = 0.0001$) (Fig. 2b) compared to that of untreated animals. Also, the colon wall comprising the crypts of Lieberkühn with underlying tissue was reduced to 122 μm (day 1) and 81 μm (day 10) in antibiotic-treated animals and antibiotic-treated animals inoculated with E980 (94 μm) or E1162 (105 to 92 μm; $P = 0.0001$, respectively), compared to that of untreated animals (146 to 143 μm, days 1 and 10) or untreated mice inoculated with E980 (160 μm; $P = 0.01$) or E1162 (146 to 122 μm; not significant and $P = 0.001$, respectively) (Fig. 2c).

In untreated animals, the mucus layer was, on average, 56 μm (day 1) and 54 μm (day 10) and distinguishable (Fig. 2d and e; see

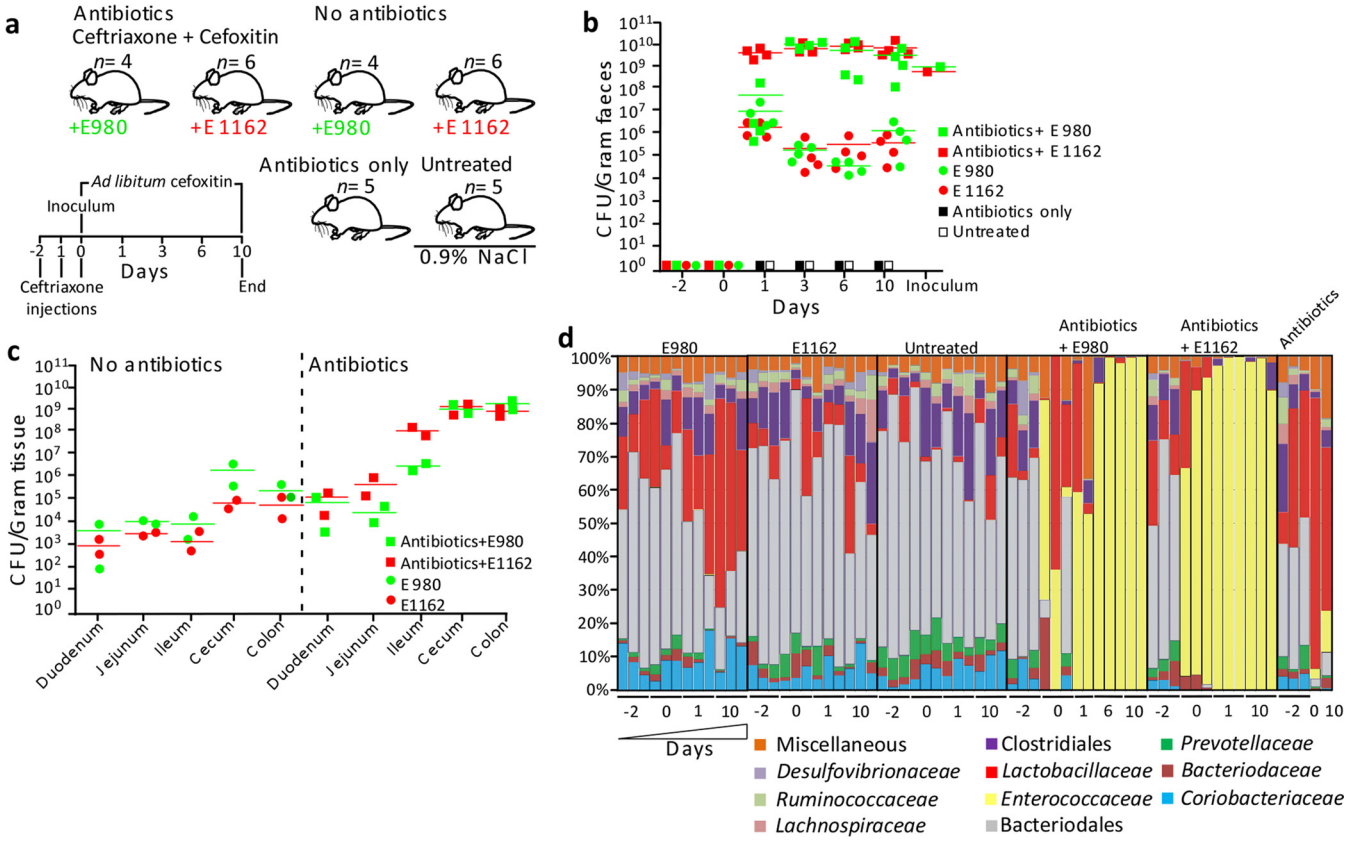

FIG 1 *E. faecium* colonization levels and 16S rRNA gene-based microbiota profiling. (a) Schematic overview of the animal model used in this study. Mice were treated with the antibiotics ceftriaxone and cefoxitin and inoculated with *E. faecium* E980 ($n = 4$) and E1162 ($n = 6$) on day 0 or treated with 0.9% NaCl and inoculated with E980 ($n = 4$) and E1162 ($n = 6$). Control mice were treated with the antibiotics only ($n = 5$) or left untreated ($n = 5$). (b, c) Quantification of *E. faecium* CFU in mouse feces ($n = 22$) (b) and in homogenized small and large intestinal parts (c) on Slanetz-Bartley agar (two mice per group). (d) Percentages of 16S rRNA gene sequences assigned to taxonomic bacterial genera present in feces during the intestinal colonization experiment. Each bar represents one mouse on 1 sampling day, and different taxa are indicated by different colors. Fecal pellets of three mice per time point were used for 16S rRNA gene sequencing. However, in some instances, not enough DNA could be extracted or the sequencing run failed. In those cases, data based on fecal pellets of only two mice per time point are shown. This was the case for antibiotic-treated mice inoculated with E980 on days 1 and 10 and mice treated with the antibiotics only on days 0, 1, and 10. For mice treated with the antibiotics and inoculated with *E. faecium* E980, an additional time point, day 6, was analyzed to compensate for the missing day 1 and 10 data.

Fig. S3 in the supplemental material). Although the mucus layer was reduced in animals inoculated with E980 (28.4 μm, day 10) or E1162 (18 to 16.2 μm, day 1 to 10; $P = 0.0001$, respectively), the layer was still visible. In contrast, the mucus layer was reduced and difficult to distinguish in antibiotic-treated animals (5.5 [day 1] to 9.8 [day 10] μm; $P = 0.0001$) and antibiotic-treated animals inoculated with E980 (19.1 μm, day 10) or E1162 (8 to 15.2 μm; $P = 0.0001$, respectively) (Fig. 2e). Analysis of colon thin sections by immunofluorescence (IF) assay with specific anti-Mucin-2 antibodies revealed a Mucin-2 layer in untreated animals, but the absence of Mucin-2 on the apical side of the epithelium in antibiotic-treated mice on day 1 (Fig. 2e) and day 10 (see Fig. S3). Complementary, Western blotting of fecal extracts obtained during the course of the experiment with specific anti-Mucin-2 antibodies revealed that Mucin-2 was present only in untreated animals and in all of the animals on day −2 (Fig. 2f). Taken together, these results indicate that antibiotic treatment greatly affects the architecture of the host's main barrier against the intestinal microbiota.

An extracellular matrix separates *E. faecium* from IECs in the antibiotic-treated host. To assess whether *E. faecium* E980 or E1162 directly interacts with the intestinal epithelium in antibiotic-treated animals, we analyzed whole cecum and colon tissue by scanning electron microscopy (SEM) and Gram-stained thin sections by light microscopy. SEM revealed that in antibiotic-treated mice diplococci were embedded in an extracellular matrix in the cecum and colon and did not directly interact with IECs (Fig. 3a). In contrast, in cecum and colon tissue sections from untreated animals and animals inoculated with either E980 or E1162, this extracellular matrix could not be detected; instead, a rod-shaped microbiota on the apical side of the epithelium was revealed (Fig. 3b). In control animals treated with only antibiotics, this extracellular matrix, in which occasionally a bacterial cell was entrapped, was also visible by SEM (Fig. 3b). Thin-section light microscopy corroborated this finding and showed that in animals treated with antibiotics and inoculated with E980 or E1162, Gram-positive (purple) cocci were detected in a thin layer on the apical side separated from the epithelium (see Fig. S4 in the supplemental material). In mice not treated with antibiotics, the microbiota was separated from the host epithelium by the intact mucus layer (Fig. 2e and Fig. S3).

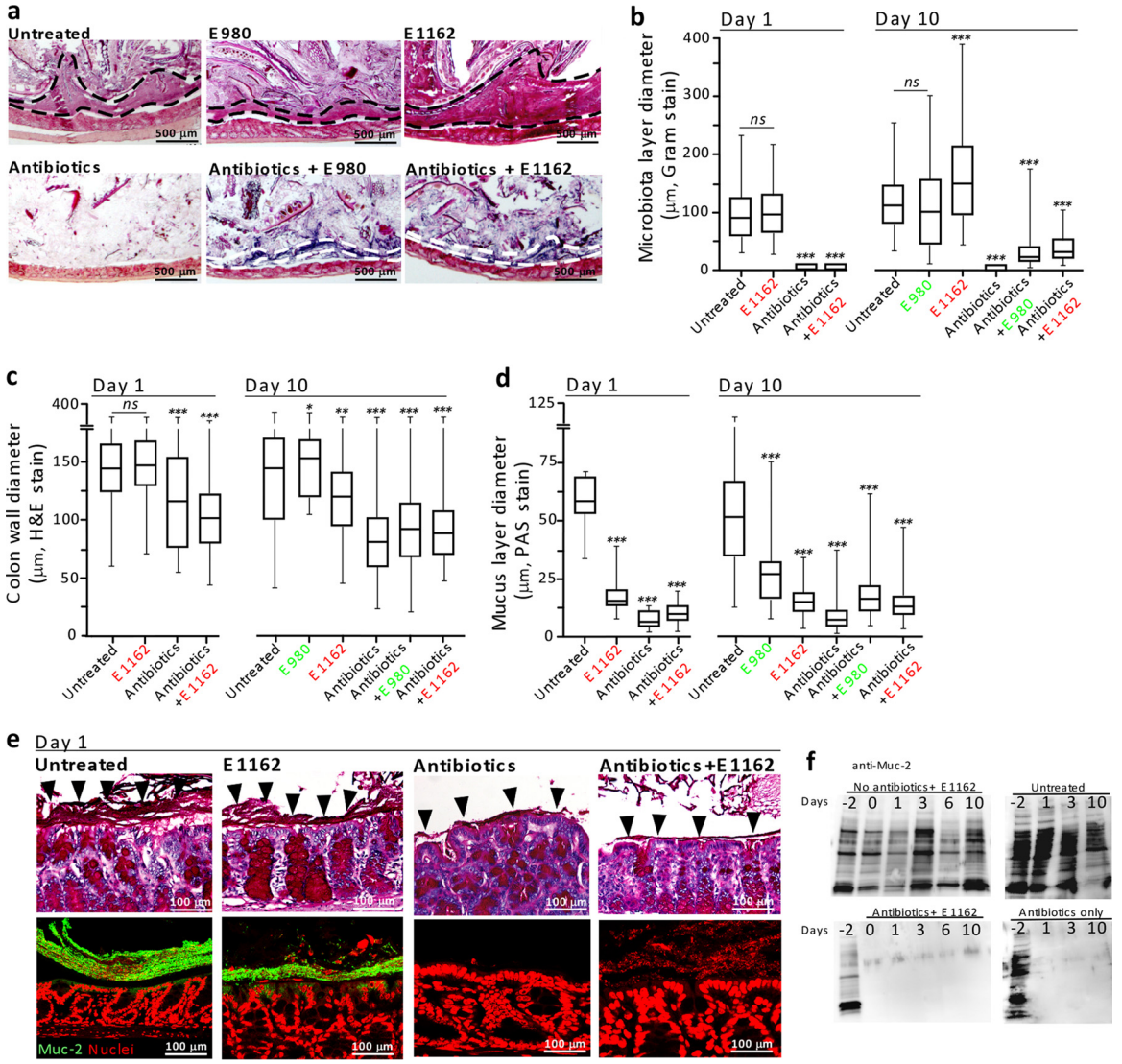

FIG 2 Alteration of intestinal architecture. (a) Images of Gram-stained colon thin sections (dashed lines mark the boundary of the microbiota; two mice per group) from day 10. (b) Quantification of the microbiota layer diameter ($n = >75$ per tissue section; two mice per group per day). (c) Quantification of the colon wall diameter ($n = >100$ per tissue section, two mice per group per day). (d) Quantification of the mucus layer diameter ($n = >150$ per tissue section; two mice per group per day). (e) Periodic acid-Schiff-stained colon thin sections (images in the top row) of mice sacrificed on day 1 (Carnoy's solution-fixed tissue). The bottom row shows IF assays of colon thin sections with anti-muc-2 antibodies. (f) Western blotting of fecal extracts of the different groups of mice and probing with anti-mucin-2 antibody. In panels b to d, each group was compared to the "untreated" control mouse group; ns, not significant; *, $P < 0.05$; **, $P < 0.001$; ***, $P < 0.0001$.

Antibiotics cause intestinal enterococcal agglutination by host determinants. To analyze determinants that constitute this extracellular matrix that segregated *E. faecium* from IECs, we punctured the ceca of mice and used their contents in IF assays (Fig. 4). Cocci could only be detected in large bacterial agglutinations in the ceca of animals treated with antibiotics and inoculated with *E. faecium* E980 or E1162 (Fig. 4a) and not in untreated control animals. In the latter, only rod-shaped bacteria were found (Fig. 4b). It is known that IgA and pIgR are secreted at high levels within the intestines (37). Therefore, we assessed whether sIgA and pIgR contribute to the agglutination of cocci in mice treated with antibiotics and inoculated with *E. faecium* E980 or E1162. IF analysis with specific anti-IgA and anti-pIgR antibodies demonstrated that IgA and pIgR were detected in the agglutinates and bound to the bacterial surface in antibiotic-treated animals that also received E980 or E1162 (Fig. 4a) and to a lesser extent to rod-shaped bacteria in untreated animals (Fig. 4c). We subsequently tested whether the adherens junction molecule E-cadherin contributes to *in vivo* agglutination (13). IF assay with anti-E-cadherin antibodies demonstrated that E-cadherin is detected in the agglutinations and binds to enterococcal surfaces. No E-cadherin signal was detected at the surface of bacteria harvested from mice inoculated with E980 or E1162 or from untreated mice (Fig. 4a to c). Animals treated with antibiotics only were not analyzed, as their ceca yielded only undigested debris. The cecum contents of four different mice incubated with conjugate alone also did not yield any signal (Fig. 4d). This suggests that E-cadherin is released in the intestinal lumen upon cephalosporin-induced dys-

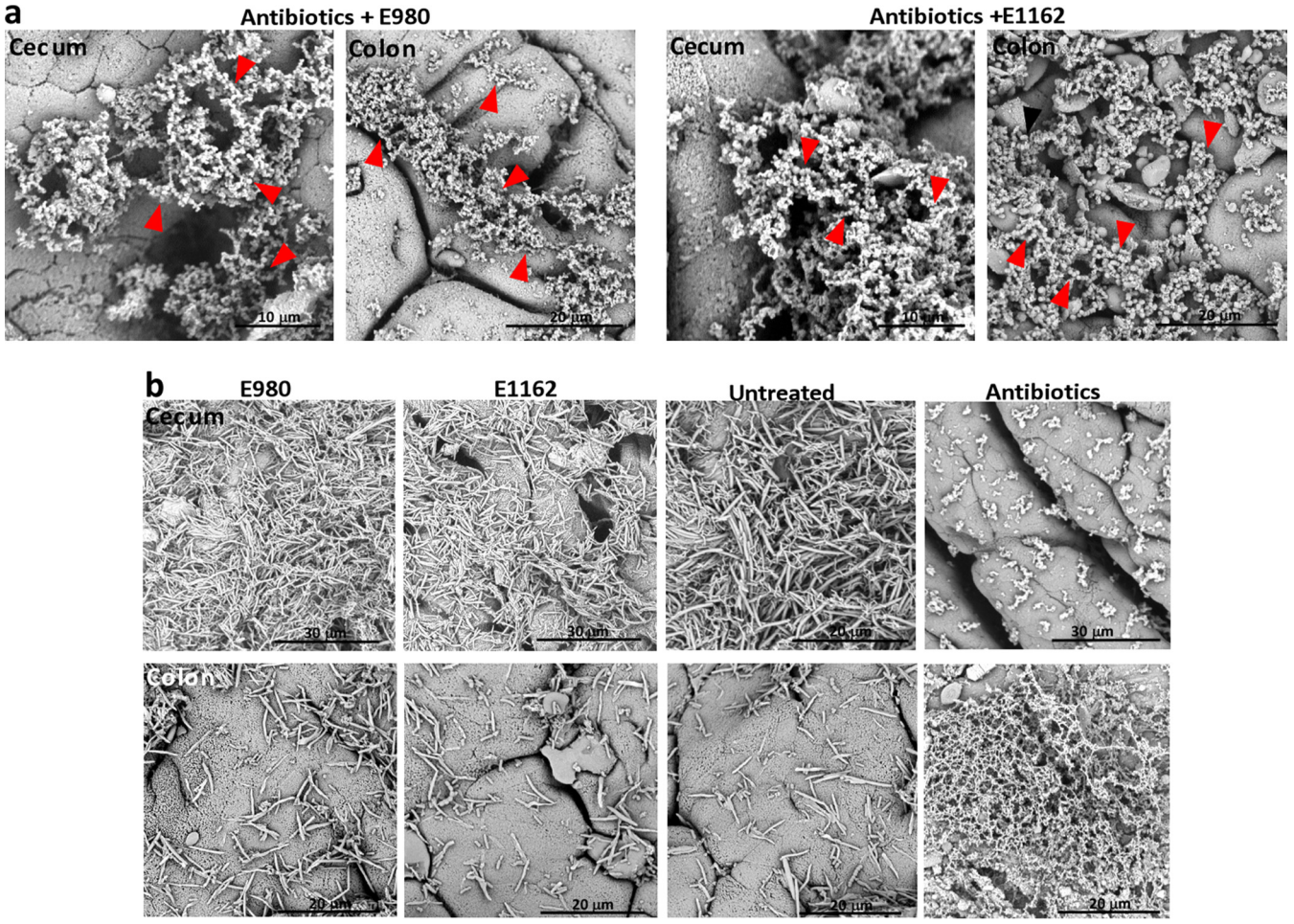

FIG 3 An extracellular matrix separates the microbiota from the host epithelium. (a) SEM of cecum and colon tissues of animals treated with cephalosporin antibiotics and inoculated with *E. faecium* E980 or E1162. (b) SEM of animals left untreated and inoculated with E980 or E1162 and control antibiotic-treated animals. Arrowheads indicate diplococci.

biosis. Accordingly, Western blotting of fecal extracts with E-cadherin antibodies showed immunoreactive E-cadherin species only in animals treated with antibiotics and not in untreated animals (Fig. 4e). Furthermore, E-cadherin labeling of adherens junctions in colon thin sections demonstrated deformed junctions in antibiotic-treated animals and normal junctions in untreated animals (Fig. 4f). To further investigate agglutination of *E. faecium* by host molecules, 20 μl of cleared and filter-sterilized fecal extracts from mice sampled at day −2 (i.e., no antibiotics) and day 1 (i.e., after 2 days of ceftriaxone injections and 1 day of cefoxitin in their drinking water of animals inoculated with E1162) were inoculated with 1×10^5 E1162 bacteria/ml. This led to agglutination of E1162 into large clumps in the day 1 fecal extract only (Fig. 4g). IF assay of these agglutinates demonstrated the presence of sIgA, pIgR, and E-cadherin as important determinants of agglutination of *E. faecium* (Fig. 4h). Lastly, 10 μg of recombinant E-cadherin, pIgR, and purified IgA proteins all agglutinated E1162 *in vitro*, as determined by IF assay, while bovine serum albumin did not (Fig. 4i). Taken together, these data show that determinants released by the host in the cecum and colon decorate the enterococcal surface, leading to intraluminal agglutination.

Enterococci are separated from the intestinal epithelium by host determinants. To analyze the relative locations of sIgA, pIgR, and E-cadherin within the cecum and colon *in vivo*, we performed IF analyses of thin sections with specific anti-IgA, anti-pIgR, and anti-E-cadherin antibodies. In all of the mouse groups, IgA^+ plasma cells were detected within the lamina propria, pIgR protein was detected on Paneth cells on the basolateral side of the crypts, and E-cadherin was detected in the adherens junctions between the cells. In antibiotic-treated animals inoculated with E1162, the E-cadherin junctions were deformed compared to those of untreated animals (Fig. 5a and b), with indications of E-cadherin shedding into the intestinal lumen. In the antibiotic-treated host inoculated with E1162, enterococci were separated from the IECs by a distinct layer consisting of the sIgA, pIgR, and E-cadherin proteins in the cecum and colon that was absent from untreated animals (Fig. 5a and b) or untreated animals inoculated with E980 or E1162 (not shown). These observations corroborate the Western blotting data in which E-cadherin was detected only in fecal extracts from mice treated with antibiotics (Fig. 4e). Close-ups showed that the sIgA, pIgR, and E-cadherin proteins were present in agglutinated E1162 clumps. This was identical in mice treated with antibiotics and inoculated with *E. faecium* E980 (data not

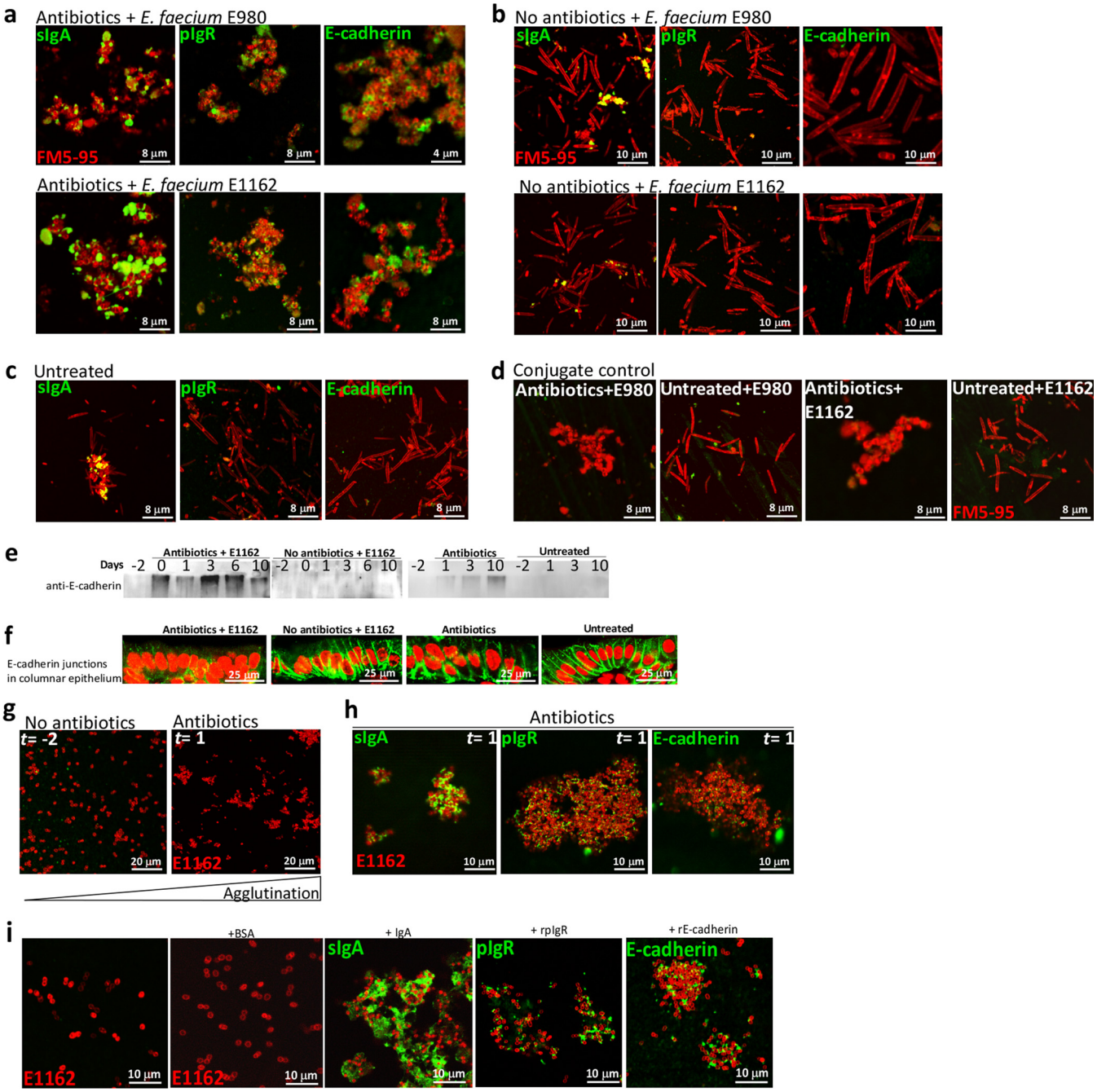

FIG 4 Agglutination of *E. faecium* by host molecules. (a) IF assays with anti-IgA, anti-pIgR, and anti-E-cadherin antibodies of the cecum contents of animals treated with antibiotics and inoculated with either E980 or E1162. (b) IF assays of the cecum contents of animals not treated with antibiotics but inoculated with either E980 or E1162 (both panels a and b are representative of two animals per group). (c) IF assays of the cecum contents of untreated animals (two animals per group). (d) Incubation of the cecum contents of antibiotic-treated and untreated mice with Alexa Fluor 488-conjugated donkey anti-goat IgG ($n = 4$). (e) Western blotting of fecal extracts with anti-E-cadherin antibodies indicating anti-E-cadherin immunoreactive species in antibiotic-treated animals only and not in untreated animals. (f) E-cadherin labeling of adherens junctions in colon thin sections demonstrating aberrant and deformed junctions in antibiotic-treated animals and normal junctions in untreated animals. (g) Agglutination of *E. faecium* E1162 in fecal extracts from day −2 (no antibiotics) and day 1 (2 days of antibiotics). (h) IF assay of these agglutinated E1162 bacteria with specific anti-IgA, anti-pIgR, and anti-E-cadherin antibodies. (i) Agglutination of *E. faecium* E1162 by recombinant IgA, pIgR, and E-cadherin proteins and not by bovine serum albumin.

shown). Animals that were treated with antibiotics but did not receive *E. faecium* showed a comparable lining of sIgA, pIgR, and E-cadherin physically separated from IECs, in particular in the colon and to a lesser extent in the cecum (Fig. 5c). Thin sections incubated with conjugate did not show a signal (Fig. 5d).

Increased Ca^{2+} levels trigger deformation of E-cadherin junctions and entrapment of *E. faecium* in an extracellular matrix *in vitro*. An elevated Ca^{2+} concentration may trigger metalloprotease-mediated E-cadherin cleavage and release (38), as we have observed in the ceca and colons of mice treated with

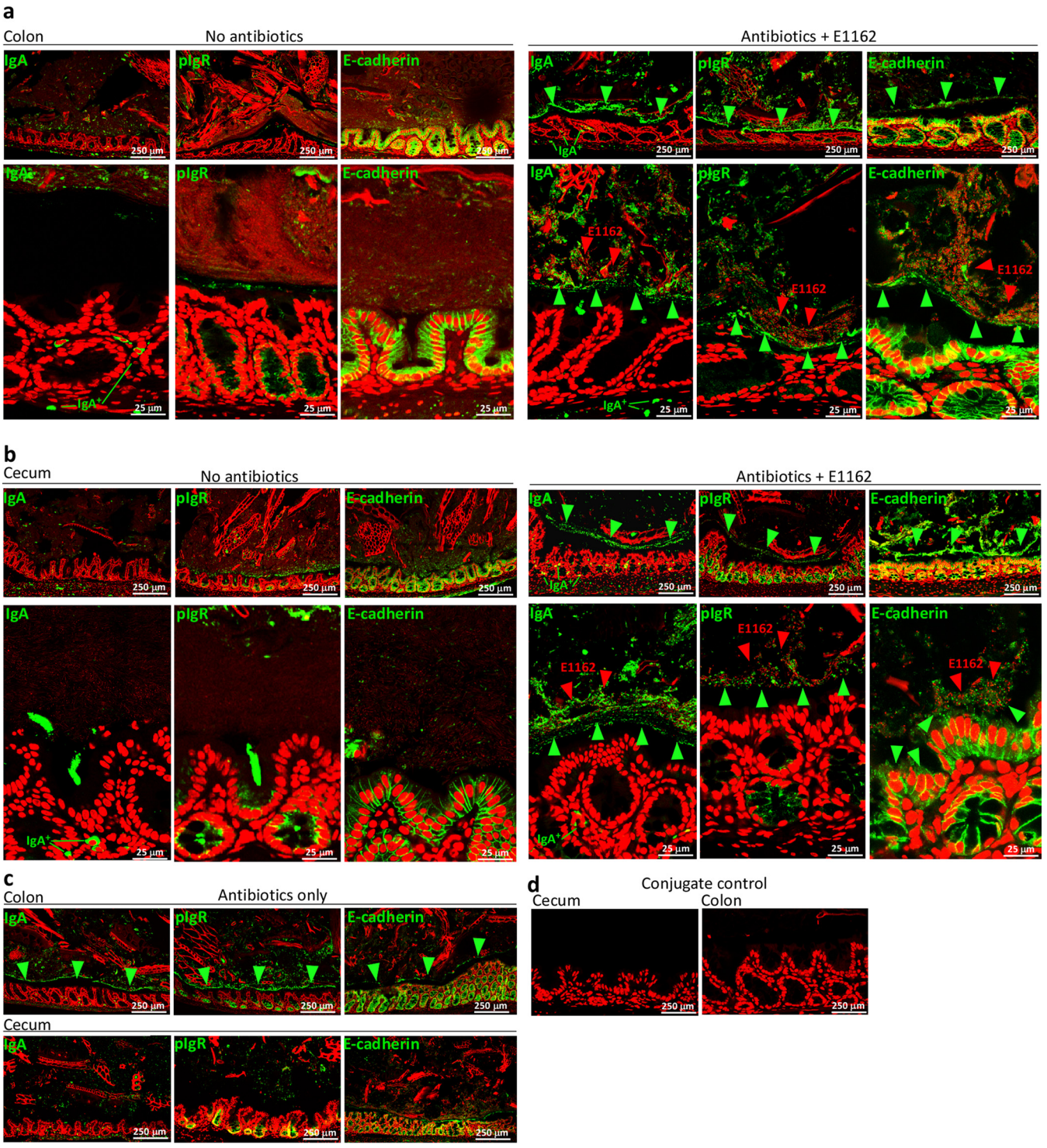

FIG 5 Visualization of agglutinations separating *E. faecium* from the host epithelium during antibiotic treatment. (a) IF assays of colon thin sections of untreated animals (left) and animals treated with antibiotics and inoculated with E1162 by using specific anti-IgA, anti-pIgR, and anti-E-cadherin antibodies (right). (b) IF assays of cecum thin sections similar to those in panel a. IgA, pIgR, and E-cadherin (green) are detected in antibiotic-treated animals in agglutinates forming a separate lining segregating the microbiota from the epithelium (green arrowheads). E1162 (red and indicated by red arrowheads) are found on the apical side of the colonic and cecum epithelium in the IgA, pIgR, and E-cadherin agglutinates. (c) Control antibiotic-treated animals also showing this physical separation lining especially in the colon (green arrowheads) and to a lesser extent in the cecum. (d) Incubation of cecum and colon thin sections with only Alexa Fluor 488-conjugated donkey anti-goat IgG did not reveal any signal. The images in panels a to d are representative of two animals per group.

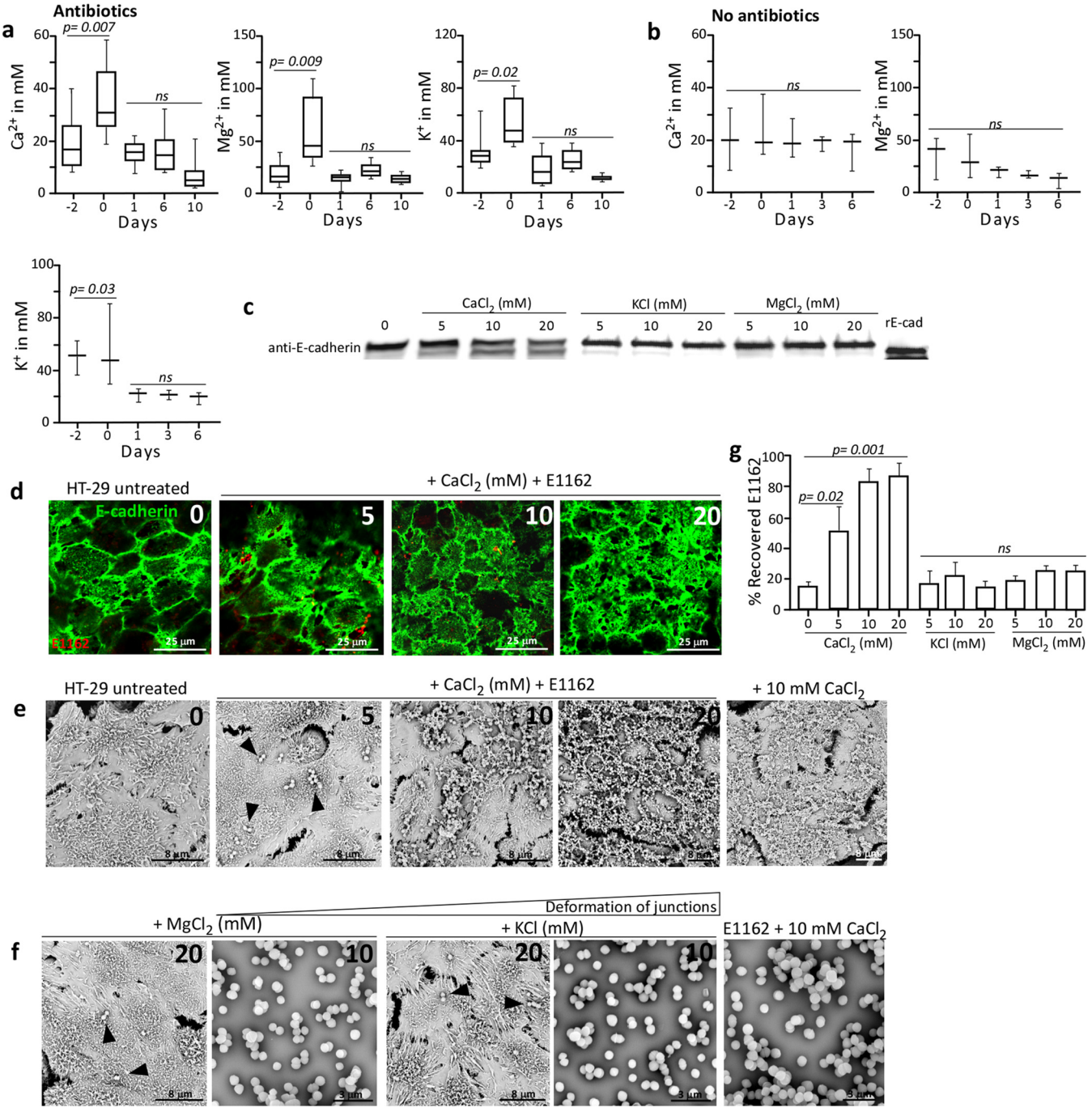

FIG 6 Cation levels, E-cadherin cleavage, and adherence of enterococci to deformed junctions. (a, b) Calcium, magnesium, and potassium concentrations determined in antibiotic-treated animals ($n = 8$) (a) and in untreated control animals ($n = 3$) (b). (c) Western blotting of HT-29 cell extracts demonstrating E-cadherin cleavage in the presence of elevated Ca^{2+} concentrations. (d) IF assays with specific anti-E-cadherin antibodies of HT-29 monolayers incubated with E1162 and increasing Ca^{2+} concentrations. (e) SEM analysis of HT-29 monolayers incubated in increasing Ca^{2+} concentrations with and without E1162 (arrowheads). (f) No extracellular matrix/deformed junctions are detected in the presence of increasing concentrations of Mg^{2+} and K^+ and the presence of E1162 (arrowheads) on HT-29 cells or by E1162 alone in the presence of 10 mM Ca^{2+}, Mg^{2+}, or K^+. Images representative of two independent experiments are shown. (g) Increased percent recovery of *E. faecium* E1162 added to HT-29 monolayers versus the inoculum in the presence of different concentrations of Ca^{2+}, K^+, and Mg^{2+}. Values are averages of three independent experiments. ns, not significant.

antibiotics. Therefore, we assessed the Ca^{2+}, Mg^{2+}, and K^+ ion concentrations in fecal extracts for their relative abundance in the intestines of antibiotic-treated mice. This demonstrated that after 2 days of ceftriaxone injections of mice, the fecal Ca^{2+} ion concentration significantly ($P = 0.007$) increased from 20 mM on day −2 to 35.5 mM on day 0 and decreased to normal levels from day 1 until day 10 (Fig. 6a). Also, fecal Mg^{2+} and K^+ ion concentrations increased from 16.6 to 58.4 mM ($P = 0.009$) and from 31.2

to 54.5 mM ($P = 0.002$), respectively, and stabilized again from day 1 to day 10. Untreated animals did not display this transient increase in fecal cation concentrations, as their Ca^{2+} concentrations were stable at 20 mM, their Mg^{2+} concentrations were stable at, on average, 25.2 mM, and their K^+ concentrations decreased from 48 to 20 mM ($P = 0.03$) (Fig. 6b). Increased Ca^{2+} concentrations might be a reflection of the altered intestinal pathophysiology, as observed in mice treated with antibiotics, involving enlargement of the cecum and diarrheic fecal contents (see Fig. S5 in the supplemental material). This suggests that cations may act as signaling molecules in the gut during antibiotic treatment and induce the formation of bacterium-host molecule agglutinates. Therefore, we analyzed E-cadherin cleavage and agglutination of *E. faecium* E1162 on monolayers of human colon HT-29 cells in the presence of different cation concentrations. By Western blotting of HT-29 cell extracts, we demonstrated that 5, 10, and 20 mM Ca^{2+} concentrations led to cleavage of E-cadherin while the other cations did not (Fig. 6c). To confirm this, an IF assay with specific anti-E-cadherin antibodies on HT-29 monolayers incubated with E1162 showed concentration-dependent deformation of the adherens junctions and E-cadherin disposition on the apical side of HT-29 cells (Fig. 6d). Similarly, SEM of HT-29 monolayers incubated with *E. faecium* E1162 and increasing Ca^{2+} concentrations showed the formation of an extracellular matrix in which E1162 was entrapped (Fig. 6e), while $MgCl_2$ or KCl concentrations of up to 20 mM did not (Fig. 6f). As a control, addition of either 10 mM $CaCl_2$ or E1162 alone to HT-29 monolayers demonstrated that calcium triggers the deformation of junctions, leading to the production of an extracellular matrix and not *E. faecium* E1162 (Fig. 6e and f). This *in vitro* deformation of junctions and Ca^{2+}-mediated production of an extracellular matrix were highly similar to those observed *in vivo* in the ceca and colons of mice treated with antibiotics (Fig. 3). Lastly, increasing Ca^{2+} concentrations correlated with increased recovery of E1162 from this extracellular matrix on HT-29 cells ($P = 0.001$) (Fig. 6g).

DISCUSSION

The mammalian intestine is densely populated by commensal bacteria, which have an essential role in metabolism and protection against invading pathogens. Antibiotic therapy is known to perturb the intestinal microbiota and to reduce colonization resistance, allowing intestinal overgrowth of multiresistant pathogens such as multiresistant *Enterococcus faecalis* (39, 40), *E. faecium* (30–32), and *Clostridium difficile* (35). Here we show in a murine model of intestinal dysbiosis that the mucus-associated microbiota and mucus layer are diminished in mice treated with cephalosporin antibiotics and that *E. faecium* is agglutinated in an extracellular matrix consisting of the host molecules sIgA, pIgR, and E-cadherin. In this way, *E. faecium*, which is able to colonize the intestines of antibiotic-treated hosts at high densities, remains physically separated from the IECs.

We assessed the antibiotic-induced alterations in microbiota composition and *E. faecium* outgrowth by 16S rRNA gene sequencing from feces in a mouse colonization model. We showed that upon cephalosporin antibiotic treatment and oral inoculation, two different *E. faecium* strains, E980 and E1162, are able to proliferate in the gastrointestinal tract. This is in line with what is found in particular categories of hospitalized patients treated with antibiotics (30, 31). Hospitalized patients densely colonized by multiresistant *E. faecium* in the gut generally do not suffer from intestinal inflammation, and enterococcal colonization typically occurs unnoticed, suggesting adequate mucosal immune responses. In our mouse model, antibiotic-induced perturbation of the microbiota not only provoked high-density intestinal outgrowth of *E. faecium* but also resulted in an altered intestinal architecture characterized by (i) a reduced mucus-associated microbiota layer, (ii) a decreased colon wall diameter, (iii) a diminished mucus layer and Mucin-2 protein production, and (iv) deformation of the E-cadherin adherens junctions. Despite this, we did not observe direct attachment of *E. faecium* cells to IECs or translocation of *E. faecium* into the lamina propria, as previously demonstrated for *E. faecalis* (41). Instead, we detected agglutinates that entrapped *E. faecium* and separated the enterococci from the underlying epithelium. These agglutinations formed an extracellular matrix located on the apical side of the intestinal epithelium and consisted of not only entrapped enterococci but also the host molecules sIgA, pIgR, and E-cadherin. sIgA containing bound pIgR and free luminal pIgR are known to protect the host against pathogenic infections and contribute to maintenance of immune homeostasis within the intestine (37). However, the abilities of sIgA and pIgR to create spatial separation and protect the host IECs from opportunistic pathogens colonizing at high density has not been attributed to their function yet. The finding of soluble luminal E-cadherin protein contributing to agglutination of *E. faecium* in the extracellular matrix is also a novel observation. So far, it has been shown that soluble E-cadherin can be detected in the blood or urine of patients affected by breast, gastric, or colorectal cancer, and this has been associated with metastatic disease and a worse prognosis (42, 43). In line with the detection of soluble luminal E-cadherin is the observation that the adherens junctions in the colonic columnar epithelium were deformed *in vivo*. This suggests that luminal E-cadherin protein has innate immune functions like sIgA and pIgR in the colonic lumen (37). Both sIgA and pIgR were also detected in colonic extracts of antibiotic-treated animals and at the surface of E980 and E1162 *in vivo*. Furthermore, inoculation of *E. faecium* into colonic fecal extracts of antibiotic-treated animals led to agglutination of enterococci by sIgA, pIgR, and E-cadherin, and the incubation of *E. faecium* with recombinant E-cadherin, sIgA, and pIgR also confirmed that these host molecules were able to agglutinate *E. faecium* while bovine serum albumin was not.

The altered architecture observed in the cecum and colon wall and at the microbiota-epithelium interface was accompanied by a transient increase in Ca^{2+}, Mg^{2+}, and K^+ concentrations in the feces of antibiotic-treated animals but not in that of untreated controls. *In vitro*, only elevated Ca^{2+} and not Mg^{2+} or K^+ leads to cleavage of E-cadherin, deformation of the E-cadherin adherens junctions, and capture of *E. faecium* E1162 in an E-cadherin matrix. This extracellular matrix was morphologically highly similar to the matrix observed in the ceca and colons of animals treated with antibiotics. Increased luminal Ca^{2+}, Mg^{2+}, and K^+ concentrations were also found in the mice after 2 days of ceftriaxone injections but were not prolonged when antibiotic treatment was changed to cefoxitin added to the drinking water of mice and when the mice were inoculated with *E. faecium*. A temporary increase in fecal metabolites (e.g., bile salts, N-acetylated amino acids, dipeptides, inositol isomers and metabolites, gamma-glutamyl amino acids) has been observed previously in mice treated with clindamycin and was attributed to the lack of uptake by the microbiota (44). This is possibly also the explanation for the

changes in intestinal cations, since we also observed additional intestinal pathophysiological changes in mice treated with antibiotics, such as an enlarged cecum and diarrhea.

We propose the following model that describes antibiotic-induced outgrowth of an opportunistic pathogen like *E. faecium* in the cecum and colon of a mammalian host (see Fig. S6 in the supplemental material). Under healthy conditions, the ceca and colons of mammals contain a diverse microbiota. Bacteria reach the outer mucus layer, but the inner mucus layer is devoid of bacteria, allowing strict separation of microbiota and IECs, colonization resistance, and immune homeostasis. This balance is further promoted by immune exclusion through the production of sIgA and pIgR at mucosal surfaces. The IEC layer forms the barrier against potentially invading bacteria, partially maintained by E-cadherin-based adherens junctions. After antibiotic administration and acquisition of a multidrug-resistant opportunistic pathogen, the microbiota of the host gets severely perturbed, leading to proliferation of *E. faecium* in the cecum and colon and a reduction of the mucus-associated microbiota and mucus layer. Furthermore, elevated Ca^{2+} concentrations, possibly resulting from perturbation of the microbiota and reduced Ca^{2+} uptake, induce E-cadherin cleavage and release and subsequent deformation of adherens junctions. We hypothesize that, upon these pathophysiological intestinal changes, the host maintains homeostasis and separates *E. faecium* from the underlying epithelium by agglutinating the bacteria in a matrix consisting of sIgA, pIgR, and E-cadherin. This may explain why patients densely colonized with multiresistant *E. faecium*, like vancomycin-resistant enterococci, in general do not suffer from intestinal inflammation. Insights into the mechanisms employed by the host to counter outgrowth by *E. faecium* may provide clues for future mucosal vaccination strategies to eradicate resistant enterococci from the intestine.

MATERIALS AND METHODS

For details of the Materials and Methods used in this study, including descriptions of the bacterial strains, mice, intestinal colonization model, antibodies, and recombinant proteins, 16S rRNA gene sequencing, 16S rRNA gene data analysis, histopathology, immunohistochemistry, cation determination assays, IF analysis, confocal microscopy, SEM, HT-29 cell culture, adherence assay, HT-29 protein extraction, *in vitro* agglutination, SDS-PAGE, Western blot analysis, and statistical analysis, see Text S1 in the supplemental material.

SUPPLEMENTAL MATERIAL

Supplemental material for this article may be found at http://mbio.asm.org/lookup/suppl/doi:10.1128/mBio.01346-15/-/DCSupplemental.

Figure S1, DOCX file, 0.2 MB.
Figure S2, DOCX file, 1.4 MB.
Figure S3, DOCX file, 2.4 MB.
Figure S4, DOCX file, 0.7 MB.
Figure S5, DOCX file, 0.2 MB.
Figure S6, DOCX file, 0.3 MB.
Text S1, DOCX file, 0.1 MB.

ACKNOWLEDGMENTS

R.J.L.W. has received funding from the European Union Seventh Framework Programme (FP7-HEALTH-2011-single-stage) under grant agreement 282004, EvoTAR.

A.P.A.H., J.T., and J.B. conceived and designed the experiments. A.P.A.H., J.T., J.B., H.K., and M.R. performed the experiments. A.P.A.H., J.T., and J.B. analyzed the data. A.P.A.H., J.B., H.K., and F.L.P. contributed reagents/materials/analysis tools. A.P.A.H., M.J.M.B., and R.J.L.W. wrote the paper.

REFERENCES

1. **Round JL, Mazmanian SK.** 2009. The gut microbiota shapes intestinal immune responses during health and disease. Nat Rev Immunol **9:**313–323. http://dx.doi.org/10.1038/nri2515.
2. **Chu H, Mazmanian SK.** 2013. Innate immune recognition of the microbiota promotes host-microbial symbiosis. Nat Immunol **14:**668–675. http://dx.doi.org/10.1038/ni.2635.
3. **Caballero S, Pamer EG.** 2015. Microbiota-mediated inflammation and antimicrobial defense in the intestine. Annu Rev Immunol **33:**227–256. http://dx.doi.org/10.1146/annurev-immunol-032713-120238.
4. **Buffie CG, Pamer EG.** 2013. Microbiota-mediated colonization resistance against intestinal pathogens. Nat Rev Immunol **13:**790–801. http://dx.doi.org/10.1038/nri3535.
5. **Vaishnava S, Yamamoto M, Severson KM, Ruhn KA, Yu X, Koren O, Ley R, Wakeland EK, Hooper LV.** 2011. The antibacterial lectin RegIIIgamma promotes the spatial segregation of microbiota and host in the intestine. Science **334:**255–258. http://dx.doi.org/10.1126/science.1209791.
6. **Cash HL, Whitham CV, Behrendt CL, Hooper LV.** 2006. Symbiotic bacteria direct expression of an intestinal bactericidal lectin. Science **313:**1126–1130. http://dx.doi.org/10.1126/science.1127119.
7. **Mathias A, Pais B, Favre L, Benyacoub J, Corthésy B.** 2014. Role of secretory IgA in the mucosal sensing of commensal bacteria. Gut Microbes **5:**688–695. http://dx.doi.org/10.4161/19490976.2014.983763.
8. **Kaetzel CS.** 2014. Cooperativity among secretory IgA, the polymeric immunoglobulin receptor, and the gut microbiota promotes host-microbial mutualism. Immunol Lett **162:**10–21. http://dx.doi.org/10.1016/j.imlet.2014.05.008.
9. **Macpherson AJ, McCoy KD, Johansen F, Brandtzaeg P.** 2008. The immune geography of IgA induction and function. Mucosal Immunol **1:**11–22. http://dx.doi.org/10.1038/mi.2007.6.
10. **Gallo RL, Hooper LV.** 2012. Epithelial antimicrobial defence of the skin and intestine. Nat Rev Immunol **12:**503–516. http://dx.doi.org/10.1038/nri3228.
11. **Turner JR.** 2009. Intestinal mucosal barrier function in health and disease. Nat Rev Immunol **9:**799–809. http://dx.doi.org/10.1038/nri2653.
12. **Rodriguez-Boulan E, Macara IG.** 2014. Organization and execution of the epithelial polarity programme. Nat Rev Mol Cell Biol **15:**225–242. http://dx.doi.org/10.1038/nrm3775.
13. **Mehta S, Nijhuis A, Kumagai T, Lindsay J, Silver A.** 2015. Defects in the adherens junction complex (E-cadherin/β-catenin) in inflammatory bowel disease. Cell Tissue Res **360:**749–760. http://dx.doi.org/10.1007/s00441-014-1994-6.
14. **Ivanov AI, Naydenov NG.** 2013. Dynamics and regulation of epithelial adherens junctions: recent discoveries and controversies. Int Rev Cell Mol Biol **303:**27–99. http://dx.doi.org/10.1016/B978-0-12-407697-6.00002-7.
15. **Johansson MEV, Sjövall H, Hansson GC.** 2013. The gastrointestinal mucus system in health and disease. Nat Rev Gastroenterol Hepatol **10:**352–361. http://dx.doi.org/10.1038/nrgastro.2013.35.
16. **McGuckin MA, Lindén SK, Sutton P, Florin TH.** 2011. Mucin dynamics and enteric pathogens. Nat Rev Microbiol **9:**265–278. http://dx.doi.org/10.1038/nrmicro2538.
17. **Johansson MEV, Phillipson M, Petersson J, Velcich A, Holm L, Hansson GC.** 2008. The inner of the two Muc2 mucin-dependent mucus layers in colon is devoid of bacteria. Proc Natl Acad Sci U S A **105:**15064–15069. http://dx.doi.org/10.1073/pnas.0803124105.
18. **Johansson MEV, Larsson JMH, Hansson GC.** 2011. The two mucus layers of colon are organized by the MUC2 mucin, whereas the outer layer is a legislator of host-microbial interactions. Proc Natl Acad Sci U S A **108**(Suppl 1):4659–4665. http://dx.doi.org/10.1073/pnas.1006451107.
19. **Cerutti A, Chen K, Chorny A.** 2011. Immunoglobulin responses at the mucosal interface. Annu Rev Immunol **29:**273–293. http://dx.doi.org/10.1146/annurev-immunol-031210-101317.
20. **Sait LC, Galic M, Price JD, Simpfendorfer KR, Diavatopoulos DA, Uren TK, Janssen PH, Wijburg OLC, Strugnell RA.** 2007. Secretory antibodies reduce systemic antibody responses against the gastrointestinal commensal flora. Int Immunol **19:**257–265. http://dx.doi.org/10.1093/intimm/dxl142.
21. **Johansen F-, Pekna M, Norderhaug IN, Haneberg B, Hietala MA, Krajci P, Betsholtz C, Brandtzaeg P.** 1999. Absence of epithelial immunoglobulin A transport, with increased mucosal leakiness, in polymeric immu-

noglobulin receptor/secretory component-deficient mice. J Exp Med **190:** 915–922. http://dx.doi.org/10.1084/jem.190.7.915.
22. **Brandtzaeg P.** 1973. Two types of IgA immunocytes in man. Nat New Biol **243:**142–143. http://dx.doi.org/10.1038/newbio243142a0.
23. **Brandtzaeg P.** 1974. Presence of J chain in human immunocytes containing various immunoglobulin classes. Nature **252:**418–420. http://dx.doi.org/10.1038/252418a0.
24. **Brandtzaeg P, Prydz H.** 1984. Direct evidence for an integrated function of J chain and secretory component in epithelial transport of immunoglobulins. Nature **311:**71–73. http://dx.doi.org/10.1038/311071a0.
25. **Sletten K, Christensen TB, Brandtzaeg P.** 1975. Human secretory component—III. Carbohydrates, amino acids and N-terminal sequence. Immunochemistry **12:**783–785. http://dx.doi.org/10.1016/0019-2791(75)90230-X.
26. **Brandtzaeg P, Fjellanger I, Gjeruldsen ST.** 1970. Human secretory immunoglobulins. I. Salivary secretions from individuals with normal or low levels of serum immunoglobulins. Scand J Haematol Suppl **12:**3–83.
27. **Brandtzaeg P, Kiyono H, Pabst R, Russell MW.** 2008. Terminology: nomenclature of mucosa-associated lymphoid tissue. Mucosal Immunol **1:**31–37. http://dx.doi.org/10.1038/mi.2007.9.
28. **Corthésy B.** 2010. Role of secretory immunoglobulin A and secretory component in the protection of mucosal surfaces. Future Microbiol **5:**817–829. http://dx.doi.org/10.2217/fmb.10.39.
29. **Hendrickx AP, van Schaik W, Willems RJ.** 2013. The cell wall architecture of *Enterococcus faecium*: from resistance to pathogenesis. Future Microbiol **8:**993–1010. http://dx.doi.org/10.2217/fmb.13.66.
30. **Ruiz-Garbajosa P, de Regt M, Bonten M, Baquero F, Coque TM, Cantón R, Harmsen HJ, Willems RJL.** 2012. High-density fecal *Enterococcus faecium* colonization in hospitalized patients is associated with the presence of the polyclonal subcluster CC17. Eur J Clin Microbiol Infect Dis **31:**519–522. http://dx.doi.org/10.1007/s10096-011-1342-7.
31. **Ubeda C, Taur Y, Jenq RR, Equinda MJ, Son T, Samstein M, Viale A, Socci ND, van den Brink MRM, Kamboj M, Pamer EG.** 2010. Vancomycin-resistant enterococcus domination of intestinal microbiota is enabled by antibiotic treatment in mice and precedes bloodstream invasion in humans. J Clin Invest **120:**4332–4341. http://dx.doi.org/10.1172/JCI43918.
32. **Brandl K, Plitas G, Mihu CN, Ubeda C, Jia T, Fleisher M, Schnabl B, DeMatteo RP, Pamer EG.** 2008. Vancomycin-resistant enterococci exploit antibiotic-induced innate immune deficits. Nature **455:**804–807. http://dx.doi.org/10.1038/nature07250.
33. **Keeney KM, Yurist-Doutsch S, Arrieta M, Finlay BB.** 2014. Effects of antibiotics on human microbiota and subsequent disease. Annu Rev Microbiol **68:**217–235. http://dx.doi.org/10.1146/annurev-micro-091313-103456.
34. **Stecher B, Maier L, Hardt W.** 2013. "Blooming" in the gut: how dysbiosis might contribute to pathogen evolution. Nat Rev Microbiol **11:**277–284. http://dx.doi.org/10.1038/nrmicro2989.
35. **Britton RA, Young VB.** 2014. Role of the intestinal microbiota in resistance to colonization by *Clostridium difficile*. Gastroenterology **146:** 1547–1553. http://dx.doi.org/10.1053/j.gastro.2014.01.059.
36. **Wlodarska M, Willing B, Keeney KM, Menendez A, Bergstrom KS, Gill N, Russell SL, Vallance BA, Finlay BB.** 2011. Antibiotic treatment alters the colonic mucus layer and predisposes the host to exacerbated *Citrobacter rodentium*-induced colitis. Infect Immun **79:**1536–1545. http://dx.doi.org/10.1128/IAI.01104-10.
37. **Brandtzaeg P.** 2013. Secretory IgA: designed for anti-microbial defense. Front Immunol **4:**222. http://dx.doi.org/10.3389/fimmu.2013.00222.
38. **Ito K, Okamoto I, Araki N, Kawano Y, Nakao M, Fujiyama S, Tomita K, Mimori T, Saya H.** 1999. Calcium influx triggers the sequential proteolysis of extracellular and cytoplasmic domains of E-cadherin, leading to loss of beta-catenin from cell-cell contacts. Oncogene **18:**7080–7090. http://dx.doi.org/10.1038/sj.onc.1203191.
39. **van der Heijden KM, van der Heijden IM, Galvao FH, Lopes CG, Costa SF, Abdala E, D'Albuquerque LA, Levin AS.** 2014. Intestinal translocation of clinical isolates of vancomycin-resistant *Enterococcus faecalis* and ESBL-producing *Escherichia coli* in a rat model of bacterial colonization and liver ischemia/reperfusion injury. PLoS One **9:**e108453. http://dx.doi.org/10.1371/journal.pone.0108453.
40. **Rigottier-Gois L, Madec C, Navickas A, Matos RC, Akary-Lepage E, Mistou M-, Serror P.** 2015. The surface rhamnopolysaccharide Epa of *Enterococcus faecalis* is a key determinant of intestinal colonization. J Infect Dis **211:**62–71. http://dx.doi.org/10.1093/infdis/jiu402.
41. **Steck N, Hoffmann M, Sava IG, Kim SC, Hahne H, Tonkonogy SL, Mair K, Krueger D, Pruteanu M, Shanahan F, Vogelmann R, Schemann M, Kuster B, Sartor RB, Haller D.** 2011. *Enterococcus faecalis* metalloprotease compromises epithelial barrier and contributes to intestinal inflammation. Gastroenterology **141:**959–971. http://dx.doi.org/10.1053/j.gastro.2011.05.035.
42. **Repetto O, De Paoli P, De Re V, Canzonieri V, Cannizzaro R.** 2014. Levels of soluble E-cadherin in breast, gastric, and colorectal cancers. Biomed Res Int **2014:**408047. http://dx.doi.org/10.1155/2014/408047.
43. **De Wever O, Derycke L, Hendrix A, De Meerleer G, Godeau F, Depypere H, Bracke M.** 2007. Soluble cadherins as cancer biomarkers. Clin Exp Metastasis **24:**685–697. http://dx.doi.org/10.1007/s10585-007-9104-8.
44. **Jump RLP, Polinkovsky A, Hurless K, Sitzlar B, Eckart K, Tomas M, Deshpande A, Nerandzic MM, Donskey CJ.** 2014. Metabolomics analysis identifies intestinal microbiota-derived biomarkers of colonization resistance in clindamycin-treated mice. PLoS One **9:**e101267. http://dx.doi.org/10.1371/journal.pone.0101267.